Evolving imaging techniques for the assessment of cardiac structure and function and their potential clinical applications

Shanks, M.

CHAPTER 10

Comparison of Aortic Root Dimensions and Geometries Pre- and Post-Transcatheter Aortic Valve Implantation by 2- and 3-Dimensional Transesophageal Echocardiography and Multi-slice Computed Tomography

Arnold C.T. Ng, Victoria Delgado, Frank van der Kley, Miriam Shanks, Nico R.L. van de Veire, Matteo Bertini, Gaetano Nucifora, Rutger J. van Bommel, Laurens F. Tops, Arend de Weger, Giuseppe Tavilla, Albert de Roos, Lucia J. Kroft, Dominic Y. Leung, Joanne Schuijf, Martin J. Schalij, Jeroen J. Bax

Circ Cardiovasc Imaging 2010;3:94-102

ABSTRACT

Objectives: Three-dimensional (3D) transesophageal echocardiography (TEE) may provide more accurate aortic annular and left ventricular outflow tract (LVOT) dimensions and geometries compared to 2-dimensional (2D) TEE. We assessed agreements between 2D-, 3D-TEE measurements with multi-slice computed tomography (MSCT), and changes in annular/LVOT areas and geometries after transcatheter aortic valve implantations (TAVI).

Methods and Results: 2D circular ($\pi \times r^2$), 3D circular and 3D planimetered annular and LVOT areas by TEE were compared to "gold standard" MSCT planimetered areas before TAVI. Mean MSCT planimetered annular area was 4.65 ± 0.82cm^2 before TAVI. Annular areas were underestimated by 2D-TEE circular (3.89 ± 0.74cm^2, $p < 0.001$), 3D-TEE circular (4.06 ± 0.79cm^2, $p < 0.001$), and 3D-TEE planimetered annular areas (4.22 ± 0.77cm^2, $p < 0.001$). Mean MSCT planimetered LVOT area was 4.61 ± 1.20cm^2 before TAVI. LVOT areas were underestimated by 2D-TEE circular (3.41 ± 0.89cm^2, $p < 0.001$), 3D-TEE circular (3.89 ± 0.94cm^2, $p < 0.001$), and 3D-TEE planimetered LVOT areas (4.31 ± 1.15cm^2, $p < 0.001$). 3D-TEE planimetered annular and LVOT areas had the best agreement with respective MSCT planimetered areas. After TAVI, MSCT planimetered (4.65 ± 0.82 vs. 4.20 ± 0.46cm^2, $p < 0.001$) and 3D-TEE planimetered (4.22 ± 0.77 vs. 3.62 ± 0.43cm^2, $p < 0.001$) annular areas decreased, whereas MSCT planimetered (4.61 ± 1.20 vs. 4.84 ± 1.17cm^2, $p = 0.002$) and 3D-TEE planimetered (4.31 ± 1.15 vs. 4.55 ± 1.21cm^2, $p < 0.001$) LVOT areas increased. Aortic annulus and LVOT became less elliptical after TAVI.

Conclusions: Before TAVI, 2D and 3D-TEE aortic annular/LVOT circular geometric assumption underestimated the respective MSCT planimetered areas. After TAVI, 3D-TEE and MSCT planimetered annular areas decreased as it assumes the internal dimensions of the prosthetic valve. However, planimetered LVOT areas increased due to a more circular geometry.

INTRODUCTION

Transcatheter aortic valve implantation (TAVI) has been demonstrated to be a feasible therapeutic alternative for high-risk surgical patients with symptomatic aortic stenosis.[1-3] Non-invasive cardiac imaging plays a central role in TAVI as pre-operative accurate measurements of aortic annular sizes are crucial for selection of appropriate prosthesis sizes. Currently, aortic annular and LVOT dimensions are assessed by 2-dimensional (2D) transthoracic or transesophageal (TEE) echocardiography. However, compared to multi-slice computed tomography (MSCT) and 3-dimensional (3D) echocardiography, 2D echocardiography underestimates the aortic annular and LVOT dimensions.[4, 5] As the use of real-time 3D-TEE to guide cardiac interventions has increased over the last few years, this imaging technique may constitute a valuable imaging tool during TAVI such as providing more accurate measurements of the aortic root and geometry. However, agreements between 3D-TEE and MSCT derived aortic annular and LVOT measurements are unknown. In addition, geometric changes in the aortic root after TAVI are unknown and may have important clinical implications during follow-up management of these patients. Thus, the aims of this study were: 1) compare aortic annular and LVOT areas derived from 2D- and 3D-TEE versus MSCT planimetered areas as “gold standard”; 2) determine agreements between TEE and MSCT derived aortic annular and LVOT areas; and 3) examine changes in aortic annular and LVOT geometries after TAVI.

METHODS

Patient population

Fifty-three patients who underwent transcatheter aortic valve implantation (TAVI) with the Edwards-Sapien valve (Edwards Lifesciences Inc., CA, USA) for treatment of severe symptomatic aortic stenosis were prospectively included. Based on the consensus of a group of cardiothoracic surgeons and cardiologists, all these patients underwent TAVI due to excessive surgical morbidity and mortality risks from conventional aortic valve replacement. Operative risk was calculated according to the logistic EuroSCORE as previously published.[6] Similarly, selection of the transfemoral versus transapical approaches was based on consensus agreements between the surgeons and cardiologists. Briefly, the transfemoral approach is selected based on the size, tortuosity and extent of calcifications of the femoral arteries, the transcatheter aortic valve and sheath sizes to be implanted, and ease of valve positioning during the procedure. Technical descriptions for the transfemoral and transapical TAVI procedure have been previously described.[2] All the authors hereby declare that all data in the present study cohort of patients has not been previously published.

All patients clinically underwent pre-operative transthoracic echocardiography to assess left ventricular (LV) function and aortic stenosis severity, and intra-operative TEE to assist the

TAVI procedure (including evaluation of operative complications) as indicated in the position statement by the European Association of Cardio-Thoracic Surgery, European Society of Cardiology and European Association of Percutaneous Cardiovascular Interventions.[3] Similarly, pre- and post-operative MSCT were clinically performed to determine aortic root dimensions prior to selection of the appropriate prosthetic valve size and to evaluate transcatheter aortic valve deployment (including complications such as device migration and vascular injury) respectively.[3]

From the various pre-TAVI TEE images, aortic annular and LVOT areas (each comprising of calculated 2D circular area, calculated 3D circular area, and 3D planimetered area) were compared with MSCT planimetered aortic annular and LVOT areas respectively; MSCT was used as the gold standard. In addition, changes in planimetered aortic annular and LVOT areas after TAVI (as compared to baseline) were evaluated with MSCT and 3D-TEE. After TAVI, as the internal dimensions of the prosthetic valve becomes the "new effective" annulus, its internal dimensions were measured as representative of the post-TAVI aortic annular dimensions.

Transthoracic echocardiography

Transthoracic echocardiography was performed in all subjects pre-operatively at rest using commercially available ultrasound transducer and equipment (M3S probe, Vivid 7, GE-Vingmed, Horten, Norway). All images were digitally stored on hard disks for offline analysis (EchoPAC version BT 07.00, GE-Vingmed, Horten, Norway). A complete 2-dimensional, color, pulsed and continuous-wave Doppler echocardiogram was performed according to standard techniques.[7, 8] Left ventricular end-diastolic volume index (EDVI) and end-systolic volume index (ESVI) were calculated using Simpson's biplane method of discs and corrected for body surface area (BSA) and LV ejection fraction (EF) was derived.[9] Mean transaortic pressure gradient was measured by continuous-wave Doppler and aortic valve area was calculated by the continuity equation.[10]

TEE imaging

Intraoperative TEE was performed in all subjects using commercially available fully sampled matrix-array TEE transducer and ultrasound system (X7-2t Live 3D-TEE transducer, iE33, Philips Medical System, Andover, MA, USA). All images were digitally stored for offline analysis (QLAB cardiac 3DQ, Philips Medical System, Andover, MA, USA). During acquisition of full volume images, gain and compression settings were optimized to display a magnified zoomed image of the aortic root in the 30° short axis or 120° long axis view.

TEE image analysis

Measurements of the 2D-TEE aortic root dimensions were performed during early systole as recommended by the American Society of Echocardiography for quantification of stroke volume and aortic stenosis severity.[10] Determinations of 2D-TEE aortic annular and LVOT diameters were performed in the 3-chamber long axis view at approximately the 120° angle. Briefly, the

aortic annular diameter was measured from the junction of the aortic leaflet with the septal endocardium to the junction of the leaflet with the mitral valve posteriorly, using the inner edge to inner edge. The LVOT diameter was obtained 5mm into the LVOT from the level of the annulus. During the 2D-TEE image acquisition, every attempt was made to ensure the largest annulus diameter was obtained (Figure 1).

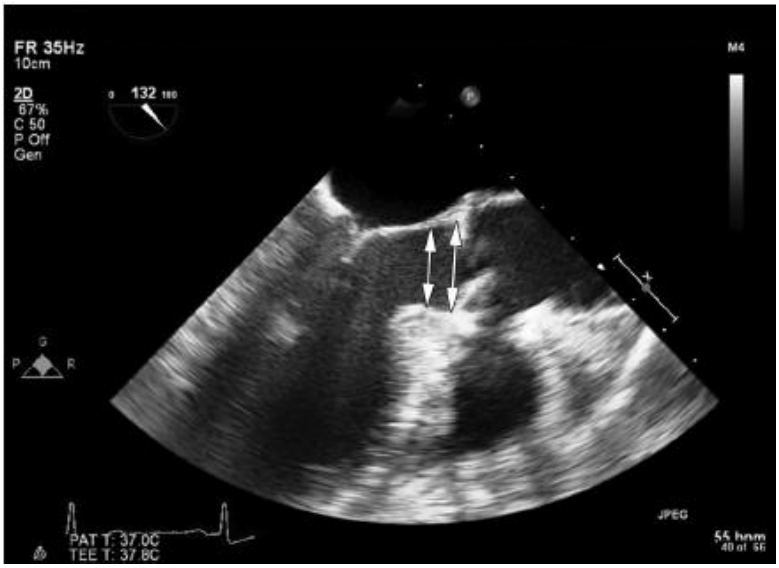

Figure 1. 2D-TEE image of the aortic root, long axis view. The aortic annular and LVOT diameters were obtained as the largest possible diameter during systole using the inner edge to inner edge as recommended by the American Society of Echocardiography. The LVOT diameter was obtained exactly 5 mm below the level of the aortic annulus.

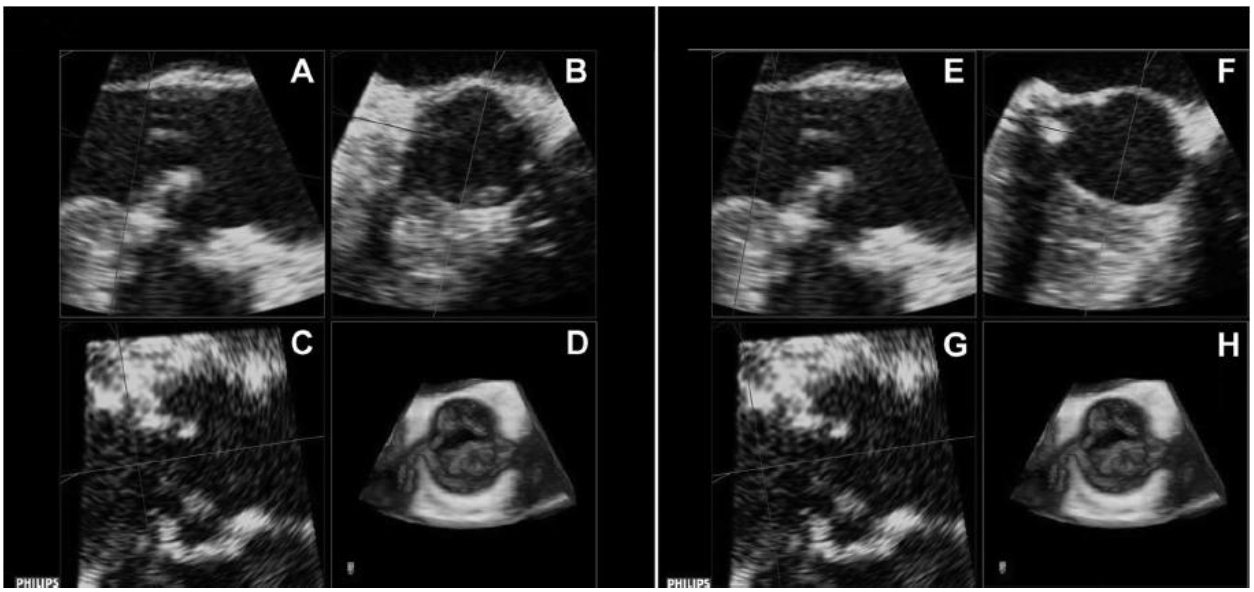

Figure 2. 3D-TEE multiplanar reformations of the aortic root. 3D-TEE circular annular and LVOT diameters were obtained as the largest possible diameter attainable in an idealized 3-chamber view (panel A and E respectively). 3D-TEE planimetered areas were obtained at the level of aortic annulus (panel B) and LVOT (panel F).

Similarly, off-line cropping of the 3D aortic root datasets were performed using 3 multi-planar reformations (MPR) planes during early systole. Cropping of the images was first performed using 2 orthogonal MPR planes bisecting the long axis of the LVOT in parallel and a third transverse plane bisecting the aortic annulus directly beneath the lowest insertion points of all 3 aortic cusps to obtain the short axis aortic annular view. The transverse MPR plane was then moved 5mm into the LVOT to obtain a representative short-axis LVOT view (Figure 2).

From the various 2D and 3D-TEE images, the following aortic annular and LVOT areas were obtained:

1. 2D circular annular area approximated by $\pi \times r^2$ (diameter derived from 3-chamber view using the 2D-TEE images);
2. 3D circular annular area approximated by $\pi \times r^2$ (diameter derived from 3-chamber view using the 3D-TEE dataset, representing the largest possible diameter obtainable in an idealized long axis view of the heart, Figure 2);
3. 3D planimetered annular area (from the 3D-TEE MPR short-axis view, Figure 2);
4. 2D circular LVOT area approximated by $\pi \times r^2$;
5. 3D circular LVOT area approximated by $\pi \times r^2$;
6. 3D planimetered LVOT area.

These aortic annular and LVOT areas from 2D and 3D-TEE were subsequently compared to the MSCT "gold standard" planimetered aortic annular and LVOT areas respectively.

MSCT imaging

All patients clinically underwent pre- and post-operative evaluations of the aortic root and transcatheter aortic valve deployment by MSCT using either a 64-slice or 320-slice MSCT scanner (Aquilion 64 and Aquilion ONE respectively, Toshiba Medical Systems, Otawara, Japan). Accordingly, data were acquired with a collimation of either 64 x 0.5 mm or 320 x 0.5 mm and a gantry rotation time of 400 ms or 350ms respectively. For the Acquilion 64, the tube current was 300 – 400 mA and the tube voltage was 120 kV or 135 kV as determined by patients' body mass indexes. Similarly for the Acquilion ONE, the tube current was 400-580 mA and tube voltage was 100 kV, 120 kV or 135 kV as determined by patients' body mass indexes.

Patient's heart rate and blood pressure were monitored prior to each scan and beta-blockers (50 to 100 mg metoprolol orally) were administered in the absence of contraindications if heart rate exceeded a threshold of 65 beats/min. All scans were performed during mid-inspiratory breath-hold and 80-90 mL of non-ionic contrast (Iomeron 400, Bracco, Milan, Italy) was injected into the antecubital vein. Subsequently, data sets were reconstructed

and off-line post-processing of MSCT images were performed on dedicated workstations (Vitrea2, Vital Images, Minneapolis, Minnesota, USA). The median time from the TAVI procedure to follow-up MSCT imaging was 1.2 months (interquartile range 1.1 – 1.9 months).

MSCT image analysis

Early systolic images of the aortic root at 30-35% of RR interval were selected and using the 3 MPR planes, a long axis image analogous to the 120° long axis view of the aortic annulus/LVOT on TEE were obtained. In a manner similar to the 3D-TEE image analysis, 2 orthogonal MPR planes bisect the long axis of the LVOT in parallel, and a third transverse plane bisects the aortic annulus directly beneath the lowest insertion points of all 3 aortic cusps to obtain the short-axis aortic annular view. The transverse MPR plane was then moved 5mm into the LVOT to obtain a representative short axis LVOT view (Figure 3). Planimetered areas for both the aortic annulus and LVOT were obtained from the various MSCT short-axis MPR views and represent the "gold standard" cross-sectional aortic annular/LVOT areas.

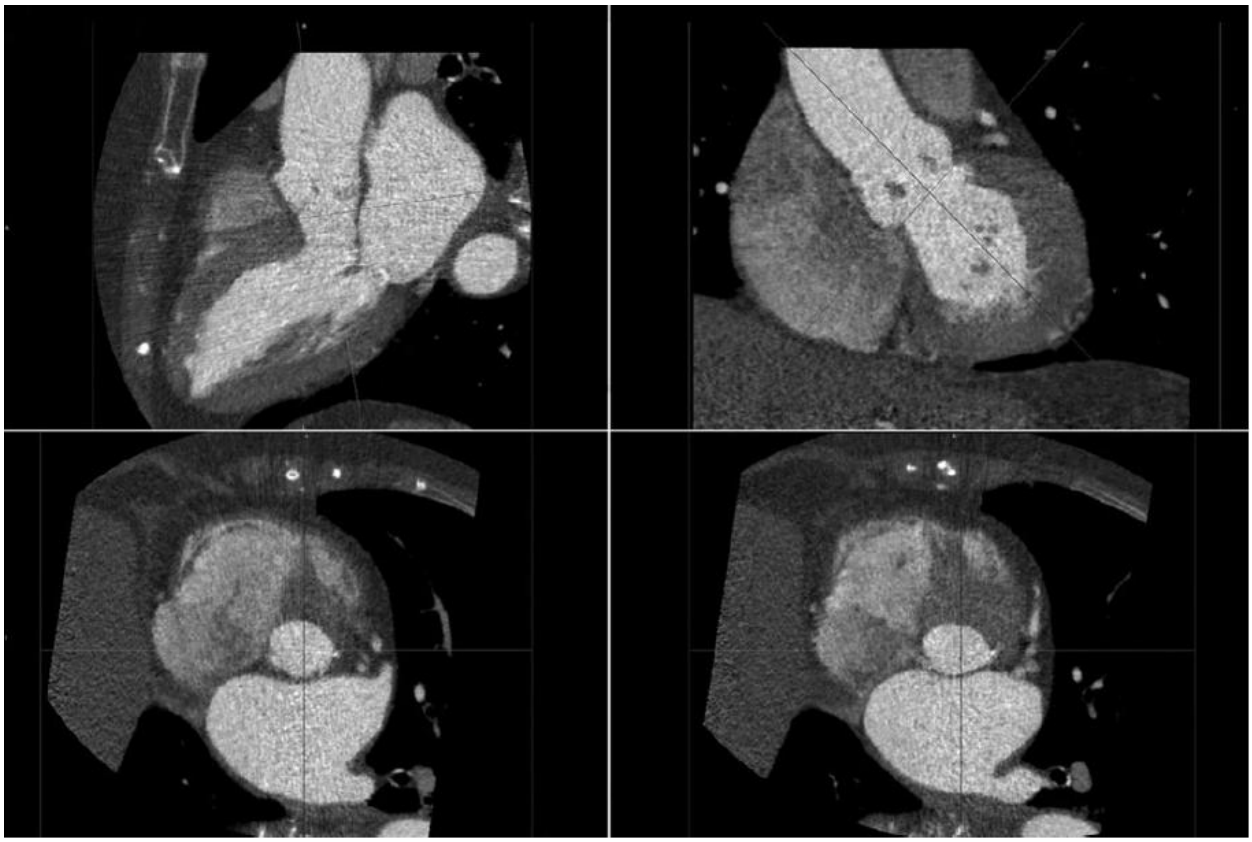

Figure 3. MSCT multiplanar reformations of the aortic root. MSCT planimetered areas were obtained at the level of aortic annulus (bottom left panel) and LVOT (bottom right panel).

Measurement of aortic annular and LVOT eccentricity

An eccentricity index was used to assess the aortic annular and LVOT geometries before and after TAVI using the short-axis MSCT and 3D-TEE images.[4] An eccentricity index of zero would represent a perfect circle while progressively higher eccentricity index represent progressively more ellipsoid geometry.

Statistical Analysis

Continuous variables were presented as mean $\pm$ 1 SD unless otherwise stated. Paired t-test was used to compare 2 groups of paired data of Gaussian distribution with Bonferroni corrections performed for multiple comparisons. Repeated measures analysis of variance (ANOVA) was used to compare ≥ 3 groups of paired data and post-hoc analysis was performed with Bonferroni correction. The method of Bland and Altman was used for agreement analysis between 2D-TEE, 3D-TEE and MSCT derived aortic annular/LVOT areas.[11] Intraobserver and interobserver agreement for TEE and MSCT derived aortic root cross-sectional areas were performed by 2 independent, blinded observers and evaluated by intraclass correlation with good agreement being defined as > 0.80. A 2-tailed p value of < 0.05 was considered significant. All statistical analyses were performed using SPSS for Windows (SPSS Inc, Chicago), version 16.

RESULTS

Baseline characteristics

The mean age was 80.0 ± 7.7 years, 28 men. Table 1 outlines the baseline clinical parameters. Mean LVEDVI, LVESVI and LVEF were 61.1 ± 27.7 mL/m^2, 32.8 ± 24.7 mL/m^2 and 51.4 ± 14.7% respectively. The mean transaortic pressure gradient and aortic valve area were 40.1 ± 16.9 mmHg and 0.69 ± 0.18 cm^2 respectively. All patients had severe aortic stenosis based on the calculated aortic valve area as indicated by current guidelines.[10] The mean logistic EuroSCORE was 21.5 ± 12.0%.

Transcatheter aortic valve implantation procedure

The transfemoral and transapical approach were performed in 31 (58.5%) and 22 (41.5%) patients respectively. The 23-mm and 26-mm Edwards-Sapien valves were successfully implanted in 12 (22.6%) and 37 (69.8%) of patients respectively. In 3 patients, the procedure was unsuccessful due to failure to advance the balloon-mounted valve across the native stenotic valve despite prior balloon dilatation, and the procedure was abandoned in 1 patient due to risk of LV apical tearing from a transapical approach. There were 3 intra-operative deaths (2 from electromechanical dissociation and 1 from extensive aortic dissection), and 4 additional patients died before hospital discharge from hemodynamic deterioration.

Table 1. Baseline Clinical Parameters of Patients

Age (years)	80.0 ± 7.7
Gender (Male/Female)	28/25
Body surface area (m^2)	1.84 ± 0.20
Co-morbidities (%)	
Diabetes mellitus	28.3
Hypertension	50.9
Smoking	18.9
Hypercholesterolemia	41.5
Positive family history	22.6
Previous myocardial infarction	26.4
Previous coronary artery bypass surgery	35.8
Aortic stenosis symptoms (%)	
Dyspnea	90.6
Angina pectoris	43.4
Syncope	1.9
Logistic EuroSCORE (%)	21.5 ± 12.0

Assessment of aortic annulus and LVOT before TAVI

Before TAVI, the mean MSCT planimetered annular area was 4.65 ± 0.82 cm^2. Cross-sectional aortic annular areas were significantly underestimated by 2D-TEE circular annular area (3.89 ± 0.74 cm^2, $p < 0.001$), 3D-TEE circular annular area (4.06 ± 0.79 cm^2, $p < 0.001$), and 3D-TEE planimetered annular area (4.22 ± 0.77 cm^2, $p < 0.001$). The method of Bland and Altman was used to assess the agreements between 2D-TEE circular annular areas versus MSCT planimetered annular areas, 3D-TEE circular annular areas versus MSCT planimetered annular areas, and 3D-TEE planimetered annular areas versus MSCT planimetered annular areas. Figure 4 shows that 3D-TEE derived planimetered annular areas had the narrowest limits of agreement and least bias. The mean difference between 2D-TEE circular annular area, 3D-TEE circular annular area and 3D-TEE planimetered annular area versus MSCT planimetered annular area were -0.77 ± 0.44 cm^2 (95% confidence interval [CI], -0.89 cm^2 to -0.64 cm^2), -0.61 ± 0.44 (95% CI, -0.73 cm^2 to -0.49 cm^2) and -0.45 ± 0.28 cm^2 (95% CI, -0.53 cm^2 to -0.37 cm^2) respectively. On average, 2D-TEE circular annular areas, 3D-TEE circular annular areas and 3D-TEE planimetered annular areas underestimated the MSCT cross-sectional annular area by 16.4%, 12.9% and 9.6% respectively.

In order to evaluate the clinical significance of underestimating the aortic annular cross-sectional areas, pre-operative aortic valve areas for all patients were re-calculated using 3D-TEE circular annular area, 3D-TEE planimetered annular area and MSCT planimetered annular area. A respective 10%, 25% and 25% of patients were re-categorized into moderate aortic stenosis based on current guidelines definition. No patients were re-categorized into mild aortic stenosis.

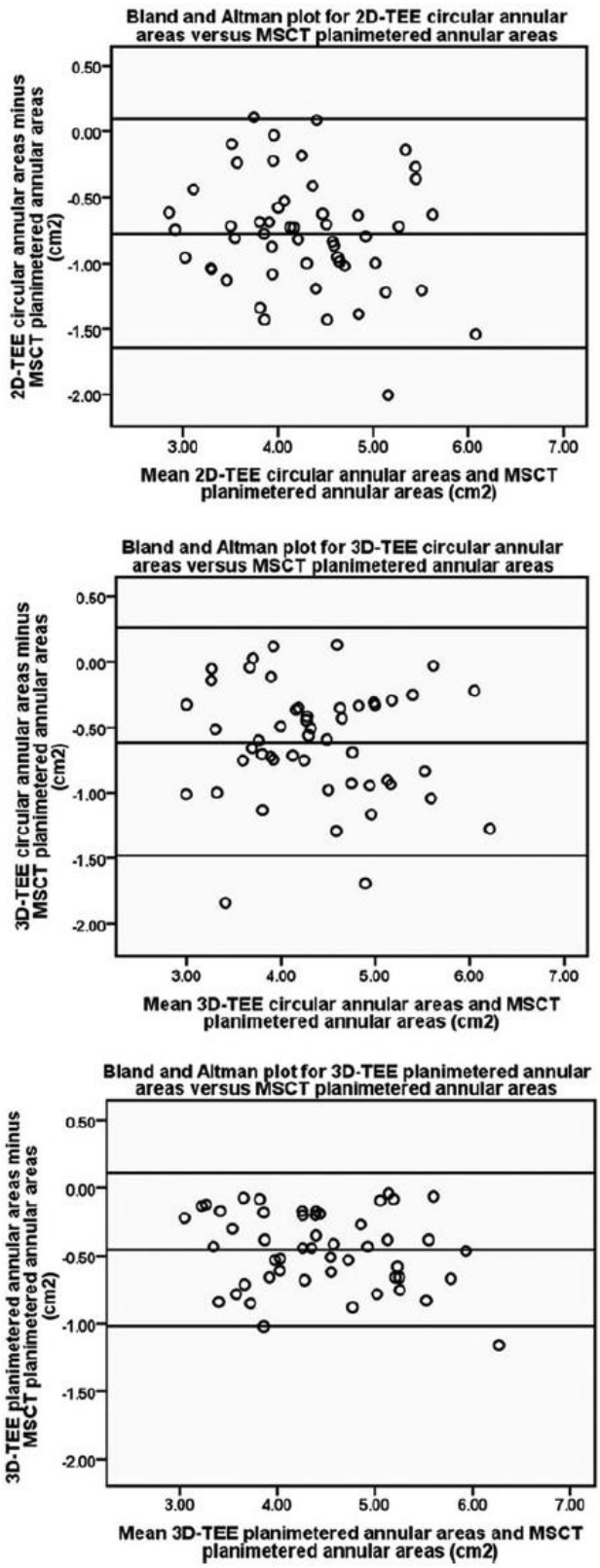

Figure 4. Bland and Altman plots comparing 2D-TEE calculated circular annular areas versus MSCT planimetered annular areas (top panel), 3D-TEE circular annular areas versus MSCT planimetered annular areas (middle panel), and 3D-TEE planimetered annular areas versus MSCT planimetered annular areas (bottom panel). 3D-TEE planimetered annular area had the narrowest limits of agreement and least bias.

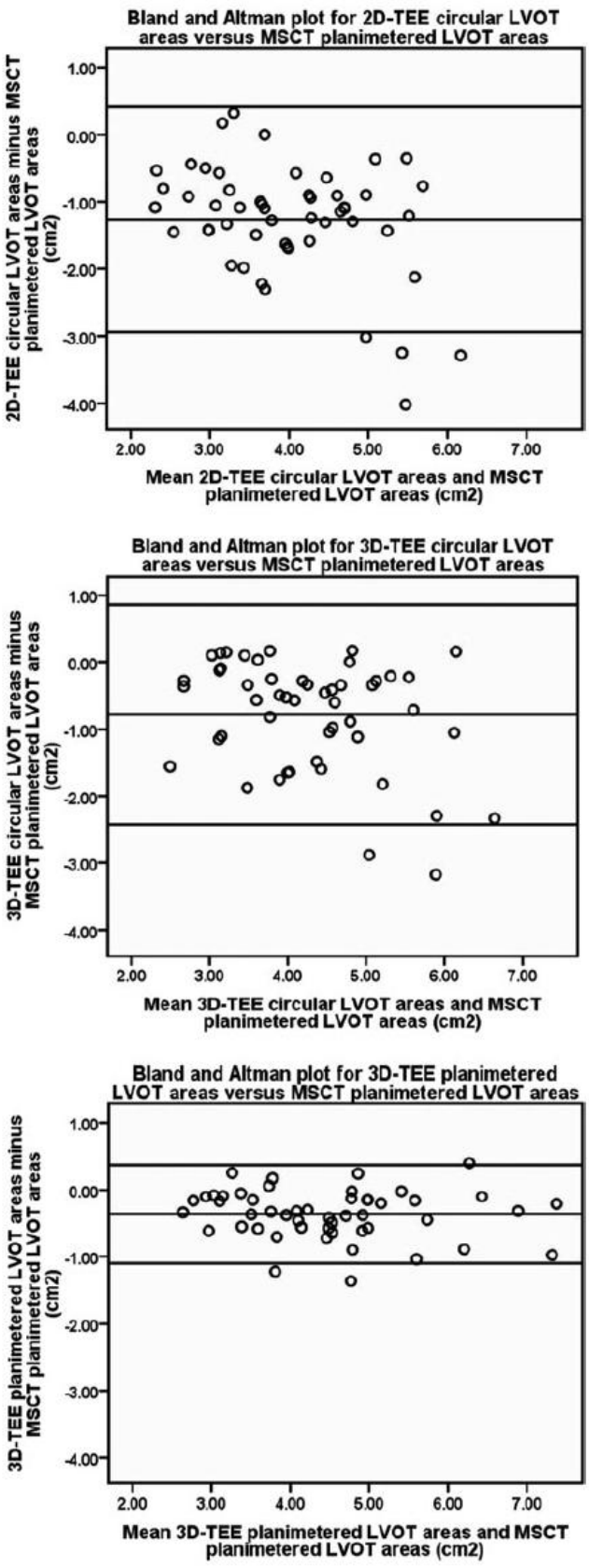

Figure 5. Bland and Altman plots comparing 2D-TEE calculated circular LVOT areas versus MSCT planimetered LVOT areas (top panel), 3D-TEE circular LVOT areas versus MSCT planimetered LVOT areas (middle panel), and 3D-TEE planimetered LVOT areas versus MSCT planimetered LVOT areas (bottom panel). 3D-TEE planimetered LVOT area had the narrowest limits of agreement and least bias.

The mean MSCT planimetered LVOT area was 4.61 ± 1.20 cm^2 before TAVI. Cross-sectional LVOT areas were significantly underestimated by 2D-TEE circular LVOT area (3.41 ± 0.89 cm^2, $p < 0.001$), 3D-TEE circular LVOT area (3.89 ± 0.94 cm^2, $p < 0.001$), and 3D-TEE planimetered LVOT area (4.31 ± 1.15 cm^2, $p < 0.001$). Similarly, the method of Bland and Altman was used to test the agreement between 2D-TEE circular LVOT areas versus MSCT planimetered annular areas, 3D-TEE circular LVOT areas versus MSCT planimetered annular areas, and 3D-TEE planimetered LVOT areas versus MSCT planimetered annular areas. 3D-TEE derived planimetered LVOT areas had the narrowest limits of agreement and least bias (Figure 5). The mean difference between 2D-TEE circular LVOT area, 3D-TEE circular LVOT area and 3D-TEE planimetered LVOT area versus MSCT planimetered LVOT area were -1.26 ± 0.84 cm^2 (95% CI, -1.50 cm^2 to -1.03 cm^2), -0.78 ± 0.82 cm^2 (95% CI, -1.01 cm^2 to -0.78 cm^2), and -0.37 ± 0.37 cm^2 (95% CI, -0.47 cm^2 to -0.26 cm^2) respectively. On average, 2D-TEE circular LVOT areas, 3D-TEE circular LVOT areas and 3D-TEE planimetered LVOT areas underestimated the MSCT cross-sectional LVOT area by 26.3%, 15.2% and 7.7% respectively.

To increase clinical utility, linear regression equations were formulated to correct for the underestimations by 2D-TEE circular annular/LVOT areas versus their respective "true" cross-sectional areas by MSCT.

$$\text{Planimetered annular area } (cm^2) = 1.01 + 0.94 \times \text{2D TEE circular annular area } (cm^2)$$
$$r = 0.85,\ p < 0.001$$

$$\text{Planimetered LVOT area } (cm^2) = 1.39 + 0.96 \times \text{2D TEE circular LVOT area } (cm^2)$$
$$r = 0.72,\ p < 0.001$$

Assessment of aortic annulus and LVOT after TAVI

After TAVI, both MSCT planimetered annular area (4.65 ± 0.82 vs. 4.20 ± 0.46 cm^2, $p < 0.001$) and 3D-TEE planimetered annular area (4.22 ± 0.77 vs. 3.62 ± 0.43 cm^2, $p < 0.001$) decreased. In contrast, both MSCT planimetered LVOT area (4.61 ± 1.20 vs. 4.84 ± 1.17 cm^2, $p = 0.002$) and 3D-TEE planimetered LVOT area (4.31 ± 1.15 vs. 4.52 ± 1.21 cm^2, $p < 0.001$) increased after TAVI.

Table 2 shows the different aortic annular/LVOT areas calculated according to various TEE methods before and after TAVI. In regards to the aortic annulus, the mean reduction in 2D-TEE circular annular area, 3D-TEE circular annular area and 3D-TEE planimetered area from pre-TAVI to post-TAVI were 0.13 ± 0.48 cm^2, 0.42 ± 0.61 cm^2, and 0.57 ± 0.58 cm^2 respectively ($p < 0.001$ by repeated measures ANOVA). Post-hoc analysis showed significant differences in the change in aortic annular areas post-TAVI between 3D-TEE circular versus 2D-TEE circular area methods ($p = 0.005$), and between 3D-TEE planimetered versus 2D-TEE circular area methods ($p < 0.001$). However, there was a non-significant trend between the 3D-TEE planimetered and

3D-TEE circular area methods (p = 0.051). In contrast, in regards to the LVOT, the mean increase in 2D-TEE circular area, 3D-TEE circular area and 3D-TEE planimetered area post-TAVI were 0.17 ± 0.57 cm2, 0.18 ± 0.85 cm2, and 0.22 ± 0.34 cm2 respectively (p = 0.73 by repeated measures ANOVA).

Table 2. Aortic annular and left ventricular outflow tract areas derived from different methods by transesophageal echocardiograms before and after transcatheter aortic valve implantations

Pre-TAVI					
Aortic annulus			LVOT		
2D TEE circular area (cm^2)	3D TEE circular area (cm^2)	3D TEE planimetered area (cm^2)	2D TEE circular area (cm^2)	3D TEE circular area (cm^2)	3D TEE planimetered area (cm^2)
3.89 ± 0.74*	4.06 ± 0.79*	4.22 ± 0.77	3.41 ± 0.89*	3.89 ± 0.94*	4.31 ± 1.15
Post-TAVI					
3.71 ± 0.53	3.60 ± 0.44	3.62 ± 0.43	3.49 ± 0.98*	4.06 ± 11.0*	4.52 ± 1.21

TAVI: transcatheter aortic valve implantation; LVOT: left ventricular outflow tract; 2D: 2-dimensional; 3D: 3-dimensional; TEE: transesophageal echocardiography. *p < 0.05 vs. respective 3D TEE planimetered annular/LVOT areas by paired t-test with Bonferroni corrections for multiple comparisons.

To assess the geometric shape change in the aortic annulus and LVOT before and after TAVI, the eccentricity index was derived using the short-axis longest and shortest diameters. Both the aortic annulus and LVOT became less elliptical after TAVI (Table 3). The mean change in aortic annular eccentricity index from pre-TAVI to post-TAVI by MSCT and 3D-TEE were 0.11 ± 0.08 and 0.08 ± 0.10 respectively. The mean change in LVOT eccentricity index from pre-TAVI to post-TAVI by MSCT and 3D-TEE were 0.05 ± 0.08 and 0.03 ± 0.07 respectively. There were no significant differences between MSCT or 3D-TEE derived eccentricity indices. Figure 6 illustrates an example of a patient with a smaller, elliptical LVOT before TAVI (left panel) and subsequent change to a less elliptical geometry after TAVI (right panel).

Table 3. Eccentricity indices for aortic annulus and left ventricular outflow tract by multislice computed tomography and 3-dimensional transesophageal echocardiography pre- and post-transcatheter aortic valve implantation

		Pre-TAVI	Post-TAVI	P value
MSCT				
	Aortic annulus	0.17 ± 0.08	0.05 ± 0.03	< 0.001
	LVOT	0.26 ± 0.09	0.20 ± 0.08	< 0.001
3D-TEE				
	Aortic annulus	0.15 ± 0.09	0.07 ± 0.05	< 0.001
	LVOT	0.24 ± 0.09	0.19 ± 0.09	0.017

TAVI: transcatheter aortic valve implantation; MSCT: multislice computed tomography; 3D-TEE: 3-dimensional transesophageal echocardiography

Intraobserver and interobserver agreements for TEE and MSCT derived cross-sectional areas were expressed by intraclass correlation and summarized in Table 4.

Table 4. Intraobserver and interobserver agreements for transesophageal and multislice computed tomography derived cross-sectional areas

Variable	Intraclass correlation
Intraobserver agreement	
2D-TEE circular area	0.952
3D-TEE circular area	0.947
3D-TEE planimetered area	0.986
MSCT planimetered area	0.988
Interobserver agreement	
2D-TEE circular area	0.911
3D-TEE circular area	0.891
3D-TEE planimetered area	0.976
MSCT planimetered area	0.994

2D: 2-dimensional; 3D: 3-dimensional; TEE: transesophageal echocardiography; MSCT: multislice computed tomography

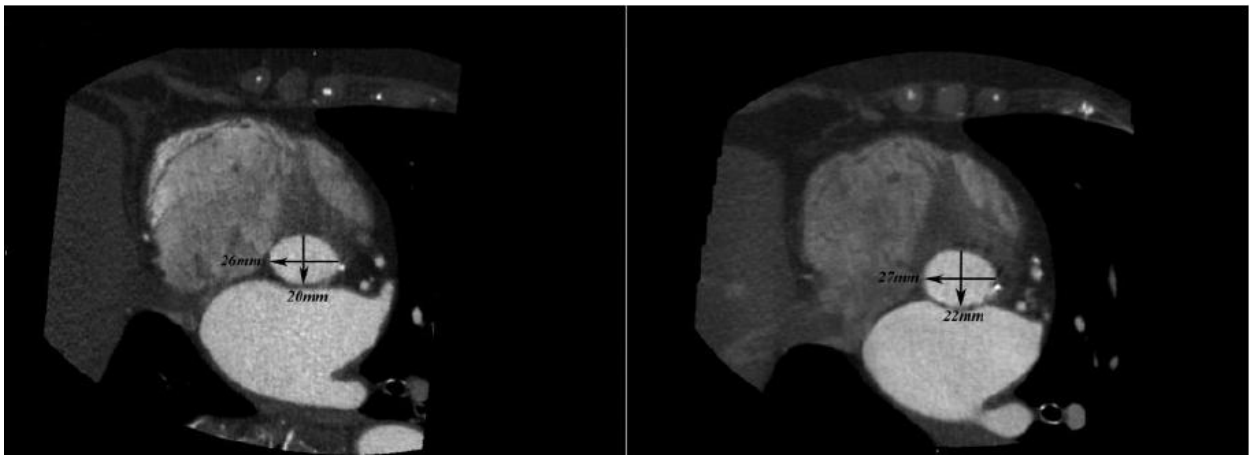

Figure 6. MSCT example of a smaller, elliptical LVOT before transcatheter aortic valve implantation (left panel, eccentricity index = 0.23) and subsequent change to a less elliptical geometry after transcatheter aortic valve implantation (right panel, eccentricity index = 0.19).

DISCUSSION

The present study demonstrated that before TAVI, the aortic annular and LVOT circular geometric assumption (by either 2D or 3D-TEE) resulted in significant underestimation of their respective MSCT planimetered areas. Using MSCT planimetered areas as “gold standard”, 3D-TEE planimetered aortic annular and LVOT areas showed the least underestimation and

narrowest limits of agreements compared to their respective calculated circular areas. After TAVI, both 3D-TEE and MSCT demonstrated significant decrease in planimetered aortic annular areas as the "new effective" aortic annulus assumes the internal dimensions of the circular prosthetic valve. In contrast, the planimetered LVOT areas increased due to a more circular geometry after TAVI.

Aortic annular and LVOT geometries and cross-sectional areas by 3D-TEE and MSCT

Current recommendations by the American Society of Echocardiography advocate either the aortic annular or LVOT diameters to be used during calculation of aortic stenosis severity by continuity equation.[10] Although caution was recommended regarding underestimating the LVOT cross-sectional area due to its elliptical geometry, no suggestions were provided to resolve any difficulties. Often in clinical practice, the aortic annular or LVOT diameters measured on TEE long axis views are clinical "gold standards" for calculating their respective circular cross-sectional areas (Figure 1). However, these echocardiographically derived diameters are often the minor diameters of an elliptically shaped annulus/LVOT, resulting in significant underestimations of the true cross-sectional areas (Figures 2 and 3). In the present study, we quantified the degree of underestimation caused by the TEE geometric assumption as ranging from 12.9% to 26.3% when compared to the respective "gold standard" MSCT planimetered areas. As the velocity time integrals do not change in the continuity equation, underestimating the aortic annular/LVOT cross-sectional areas by 12.9% to 26.3% will automatically equate to similar degrees of underestimations for the calculated aortic valve areas. Furthermore, this error in the calculation of aortic valve area is likely to be more pronounced in the presence of suboptimal images by 2D transthoracic echocardiography. This was reflected in a respective 10%, 25% and 25% of patients being reclassified as having moderate aortic stenosis based on calculated aortic valve areas using 3D-TEE circular annular area, 3D-TEE planimetered annular area and MSCT planimetered annular area.

Although 3D-TEE can avoid this geometric assumption limitation by permitting direct planimetry of the cross-sectional annular/LVOT areas, the present study demonstrated that 3D-TEE planimetered annular/LVOT areas still underestimated their respective MSCT planimetered areas by up to 9.6%. This was most likely due to a lower spatial resolution associated with 3D-TEE volumetric imaging. However, Bland-Altman analyses showed the least bias and narrowest limits of agreement when comparing planimetered annular/LVOT areas by 3D-TEE and MSCT, and the absolute difference in the planimetered annular/LVOT areas between both imaging modalities was small. In contrast, agreements were lower when comparing 2D-TEE or 3D-TEE derived circular annular/LVOT areas with their respective MSCT planimetered areas. Thus, underestimation of aortic annular/LVOT cross-sectional areas due to a lower echocardiographic spatial resolution is probably not as clinically important as the erroneous geometric assumption of a circular aortic root.

Changes in aortic annular and LVOT geometries after TAVI

In the present study, both MSCT and 3D-TEE demonstrated an elliptical aortic annular/LVOT geometry before TAVI, leading to significant underestimations of their "true" cross-sectional areas when assuming a circular geometry. However, after TAVI, the "new effective" aortic annulus assumes the smaller circular internal dimensions of the deployed prosthetic valve. Consequently, aortic annular area is smaller after TAVI, and the near circular geometry of the deployed prosthetic valve resulted in no significant difference between the calculated circular versus planimetered annular areas. In contrast, the planimetered LVOT area increased after TAVI due to a less elliptical geometry (Figure 6). However, LV reverse remodeling with regression of hypertrophy could have contributed to a larger LVOT measurement by MSCT at 1 month follow-up.

Clinical implications

Transcatheter aortic valve implantation is a feasible therapeutic alternative for high-risk surgical patients with severe symptomatic aortic stenosis.[1-3] 3D volumetric imaging by 3D-TEE is an ideal pre-operative imaging modality to assess the native aortic root dimensions prior to TAVI. The ability to non-invasively measure cross-sectional aortic annular/LVOT areas by 3D-TEE has important clinical implications such as selection of appropriate prosthetic valve size and more accurate calculations of stroke volumes. Post-operatively, as the aortic annulus assumes a more circular geometry, calculated circular annular area by transthoracic echocardiography is an accurate and inexpensive method to follow the progress of transcatheter aortic valve function.

Study limitations

One study limitation is the lack of phantom imaging by 3D TEE and MSCT to determine their "true accuracy". However, the present study was performed as part of the pre- and post-operative assessment of patients who underwent TAVI as part of their on-going clinical management. Furthermore, MSCT had superior spatial signal-to-noise ratio compared to echocardiography, and was thus used as a "clinical gold standard".

CONCLUSIONS

Before TAVI, echocardiographic assumption of a circular aortic annular/LVOT geometry leads to significant underestimation of their "true" cross-sectional area. Direct planimetry of the aortic annular/LVOT areas by 3D-TEE volumetric imaging showed the best agreement with MSCT "gold standard". After TAVI, aortic annular area decreased as the "new effective" annulus assumes the internal dimensions of the prosthetic valve whereas the LVOT area increased due to a more circular geometry. These changes can be accurately assessed by 3D-TEE.

REFERENCES

1. Grube E, Schuler G, Buellesfeld L, et al. Percutaneous aortic valve replacement for severe aortic stenosis in high-risk patients using the second- and current third-generation self-expanding CoreValve prosthesis: device success and 30-day clinical outcome. *J Am Coll Cardiol* 2007;50:69-76.
2. Rodes-Cabau J, Dumont E, De LaRochelliere R, et al. Feasibility and initial results of percutaneous aortic valve implantation including selection of the transfemoral or transapical approach in patients with severe aortic stenosis. *Am J Cardiol* 2008;102:1240-6.
3. Vahanian A, Alfieri O, Al Attar N, et al. Transcatheter valve implantation for patients with aortic stenosis: a position statement from the European Association of Cardio-Thoracic Surgery (EACTS) and the European Society of Cardiology (ESC), in collaboration with the European Association of Percutaneous Cardiovascular Interventions (EAPCI). *Eur Heart J* 2008;29:1463-70.
4. Doddamani S, Bello R, Friedman MA, et al. Demonstration of left ventricular outflow tract eccentricity by real time 3D echocardiography: implications for the determination of aortic valve area. *Echocardiography* 2007;24:860-6.
5. Doddamani S, Grushko M, Makaryus A, et al. Demonstration of left ventricular outflow tract eccentricity by 64-slice multi-detector CT. *Int J Cardiovasc Imaging* 2009;25:175-81.
6. Roques F, Michel P, Goldstone AR, et al. The logistic EuroSCORE. *Eur Heart J* 2003;24:882.
7. Nishimura R, Miller FJ, Callahan M, et al. Doppler echocardiography: theory, instrumentation technique and application. *Mayo Clin Proc* 1985;60:321-43.
8. Tajik A, Seward J, Hagler D, et al. Two dimensional real-time ultrasonic imaging of the heart and great vessels: technique, image orientation, structure identification and validation. *Mayo Clin Proc* 1978;53:271-303.
9. Mosteller RD. Simplified calculation of body-surface area. *N Engl J Med* 1987;317:1098.
10. Baumgartner H, Hung J, Bermejo J, et al. Echocardiographic assessment of valve stenosis: EAE/ASE recommendations for clinical practice. *J Am Soc Echocardiogra* 2009;22:1-23.
11. Bland JM, Altman DG. Statistical methods for assessing agreement between two methods of clinical measurement. *Lancet* 1986;1:307-10.